Euro. Jnl of Applied Mathematics: (2019), *vol.* 30, *pp.* 928–944
doi:10.1017/S0956792518000530

Approximate analytical solutions for a class of nonlinear stochastic differential equations

A. T. MEIMARIS [1], I. A. KOUGIOUMTZOGLOU [2] and A. A. PANTELOUS [1]

[1]*Department of Econometrics and Business Statistics, Monash Business School, Monash University, 20 Chancellors Walk, Wellington Road, Clayton, Victoria 3800, Australia*
emails: Antonios.Meimaris@monash.edu; Athanasios.Pantelous@monash.edu
[2]*Department of Civil Engineering and Engineering Mechanics, The Fu Foundation School of Engineering and Applied Science, Columbia University, 500 West 120th Street, New York, NY 10027, USA*
email: ikougioum@columbia.edu

(*Received 13 January 2018; revised 27 July 2018; accepted 31 July 2018; first published online 18 September 2018*)

An approximate analytical solution is derived for a certain class of stochastic differential equations with constant diffusion, but nonlinear drift coefficients. Specifically, a closed form expression is derived for the response process transition probability density function (PDF) based on the concept of the Wiener path integral and on a Cauchy–Schwarz inequality treatment. This is done in conjunction with formulating and solving an error minimisation problem by relying on the associated Fokker–Planck equation operator. The developed technique, which requires minimal computational cost for the determination of the response process PDF, exhibits satisfactory accuracy and is capable of capturing the salient features of the PDF as demonstrated by comparisons with pertinent Monte Carlo simulation data. In addition to the mathematical merit of the approximate analytical solution, the derived PDF can be used also as a benchmark for assessing the accuracy of alternative, more computationally demanding, numerical solution techniques. Several examples are provided for assessing the reliability of the proposed approximation.

Key words: Stochastic Differential Equations, Stochastic Dynamics, Path Integral, Error quantification, Cauchy-Schwarz inequality

2010 Mathematics Subject Classification: 34K50, 60H10, 60H35, 81P20, 97K60

1 Introduction

Stochastic differential equations (SDEs) have been widely used over the past decades for modelling the complex dynamics of diverse systems in a wide range of scientific disciplines. Numerical Monte Carlo simulation (MCS) methodologies such as the Euler–Maruyama and the Milstein schemes have been among the most versatile tools for solving SDEs of general form [6]. Nevertheless, in many cases they can be computationally prohibitive, and thus, there is a need for developing alternative efficient approximate analytical solution techniques. Indicative alternative approaches include stochastic averaging [20], Markov approximations and related Fokker–Planck equations, probability density evolution schemes [13], as well as numerical versions of the Chapman–Kolmogorov equation [16, 25].

One of the promising semi-analytical techniques relates to the concept of path integral, developed independently by Wiener [26] and Feynman [4]. The rationale relates to expressing the stochastic process transition probability density function (PDF) as a functional integral over the space of all possible paths [1]; see also [23] for a large deviation theory perspective on the topic. Kougioumtzoglou and co-workers extended and applied recently the technique to engineering dynamics problems, where the structural/mechanical system under consideration is typically modelled as a set of coupled nonlinear SDEs [2, 12, 10, 11]. Although the aforementioned Wiener path integral (WPI) technique has exhibited satisfactory accuracy in determining the response PDF, its numerical implementation is associated, in general, with non-negligible computational cost [12]. In this regard, the authors derived recently an approximate analytical solution PDF for a certain class of SDEs with constant diffusion, but nonlinear drift coefficients, by relying on the WPI and on a Cauchy–Schwarz inequality treatment of the problem [14].

In this paper, the accuracy exhibited by the derived approximation of [14] is enhanced by introducing a more general form for the response process PDF. This enhancement aims at 'tightening' the Cauchy–Schwarz inequality as well as increasing the overall accuracy of the basic approximation in [14]. To this aim, an optimisation problem is formulated and solved by relying on an error definition based on the Fokker–Planck equation operator. Several numerical examples are included to demonstrate the accuracy of the derived approximate PDF. Comparisons with pertinent MCS data are included as well.

2 Preliminaries

Let $(\Omega, \mathcal{F}, \mathcal{F}_{t\geq 0}, \mathbb{P})$ be a complete filtered probability space on which a scalar standard Brownian motion $(B_t, t \geq 0)$ is defined; and $\mathcal{F}_t$ is the augmentation of $\sigma\{B_s | 0 \leq s \leq t\}$ by all the $\mathbb{P}$-null sets of $\mathcal{F}$.

2.1 WPI overview

In general, for a stochastic process X_t, the transition PDF $p\left(x_f, t_f | x_i, t_i\right)$ from a point in state space x_i at time t_i to a point x_f at time t_f, where $t_f > t_i$, can be expressed as a functional integral over the space of all possible paths $C\left\{x_i, t_i; x_f, t_f\right\}$ in the form (e.g. see [1])

$$p\left(x_f, t_f | x_i, t_i\right) = \int_{\{x_i, t_i\}}^{\{x_f, t_f\}} W[x(t)][dx(t)]. \tag{2.1}$$

In (2.1), $W[x(t)]$ represents the probability density functional, which can be explicitly determined only for relatively simple cases of stochastic processes. For instance, denoting the expectation operator as $\mathbf{E}$, the probability density functional for the white noise process $v(t)$, i.e. $\mathbf{E}(v(t)) = 0$ and $\mathbf{E}(v(t_1)v(t_2)) = 2\pi S_0 \delta(t_1 - t_2)$, is given by [22]:

$$W[v(t)] = \Phi \exp\left[-\int_{t_i}^{t_f} \frac{1}{2} \frac{v(t)^2}{2\pi S_0} dt\right], \tag{2.2}$$

where Φ is a normalisation coefficient. A detailed derivation and discussion of (2.2) can be found in standard path integral-related books such as [1]. In the ensuing analysis, the SDE

$$dX_t = \mu\left(X_t\right) dt + \sigma dB_t \tag{2.3}$$

https://doi.org/10.1017/S0956792518000530 Published online by Cambridge University Press

is considered, where $\sigma^2 = 2\pi S_0$ and dB_t represents the formal time derivative of a white noise process of unit intensity. In this regard, combining (2.1)–(2.3) yields the transition PDF of the response process X_t (e.g. see [2, 12, 10, 11, 8])

$$p\left(x_f, t_f | x_i, t_i\right) = \int_{\{x_i,t_i\}}^{\{x_f,t_f\}} \Phi \exp\left(-\int_{t_i}^{t_f} L(x,\dot{x})dt\right)[dx(t)], \tag{2.4}$$

where $L(x,\dot{x})$ represents the Lagrangian function associated with the process X_t and is given by

$$L(x,\dot{x}) = \frac{1}{2\sigma^2}\left(\dot{x} - \mu(x)\right)^2. \tag{2.5}$$

Next, it is readily seen that evaluating analytically, the WPI of (2.4) is at least a rather challenging, if not impossible, task; thus, an approximate solution technique is required. To this aim, it is noted that the largest contribution to the WPI comes from the trajectory for which the integral in the exponential of (2.4) becomes as small as possible. According to calculus of variations [3], this trajectory with fixed end points satisfies the extremality condition

$$\delta \int_{t_i}^{t_f} L(x_c, \dot{x}_c)dt = 0, \tag{2.6}$$

where x_c denotes the 'most probable path' to be determined by solving the functional optimisation problem

$$Min(Max) \qquad J[x_c(t)] = \int_{t_i}^{t_f} L(x_c, \dot{x}_c)dt, \tag{2.7}$$

or alternatively, by solving the Euler–Lagrange (E–L) equation associated with (2.6) (e.g. see [2, 12]), i.e.

$$\frac{\partial L}{\partial x_c} - \frac{\partial}{\partial t}\frac{\partial L}{\partial \dot{x}_c} = 0, \tag{2.8}$$

in conjunction with the boundary conditions $x_c(t_i) = x_i$, $x_c(t_f) = x_f$. Once $x_c(t)$ is determined, the response transition PDF can be approximated by

$$p\left(x_f, t_f | x_i, t_i\right) \approx \Phi \exp\left(-\int_{t_i}^{t_f} L(x_c, \dot{x}_c)dt\right). \tag{2.9}$$

Comparing (2.4) and (2.9), it is seen that only the largest contribution to the WPI of (2.4) is considered in the approximation of (2.9); this comes from the most probable path $x_c(t)$ for which the integral in (2.7) becomes as small as possible. From a computational point of view, the numerical solution of a boundary value problem (BVP) of the form of (2.7) yields a single point of the response PDF via (2.9). Therefore, following a brute force discretisation of the response PDF domain into N points requires the solution of N BVPs of (2.7). This translates into considerable computational cost, and thus, there is merit in developing more efficient solution methodologies. This is also the scope of the present paper; see also [12] for a detailed presentation.

2.2 Cauchy–Schwarz inequality

Applications of the Cauchy–Schwarz inequality have been fruitful across many areas of mathematics and applied sciences, ranging from analysis and geometry to combinatorics, probability

https://doi.org/10.1017/S0956792518000530 Published online by Cambridge University Press

theory and statistics [7, 15]. For completeness, the integral form of the Cauchy–Schwarz inequality is included below, whereas a detailed presentation of the topic can be found in [21].

Lemma 2.1 *Let f and g be real functions that are continuous on the closed interval $[a, b]$. Then*

$$\left(\int_a^b f(t)g(t)dt\right)^2 \leq \int_a^b f(t)^2 dt \int_a^b g(t)^2 dt. \tag{2.10}$$

Clearly, setting $g = 1$ yields the special case

$$\int_a^b f(t)^2 dt \geq \frac{1}{b-a}\left(\int_a^b f(t)dt\right)^2. \tag{2.11}$$

3 Main results

3.1 Approximate solution PDF for a class of SDEs with constant diffusion and nonlinear drift coefficients

In this section, relying on the WPI-based approximation of (2.9) and on the Cauchy–Schwarz inequality of (2.11) in conjunction with an optimisation scheme, approximate non-stationary response PDFs are derived for the SDE of (2.3) at a minimal computational effort. The herein developed technique can be construed as a generalisation and enhancement from an accuracy perspective of the results presented in [14].

Considering (2.5) and (2.8), for fixed t_i, t_f yields

$$\ddot{x}_c = \mu(x_c)\frac{\partial \mu(x_c)}{\partial x_c}, \tag{3.1}$$

which, equivalently, can be transformed into

$$\dot{x}_c^2 = \mu(x_c)^2 + b, \tag{3.2}$$

where b is a constant. Following the derivation in [14], by substituting (3.2) into (2.5) and integrating yields

$$\int_{t_i}^{t_f} L(x_c, \dot{x}_c)dt = \frac{1}{2}\left(\frac{2\int_{t_i}^{t_f} \dot{x}_c{}^2 dt - b(t_f - t_i) - 2M(x_f) + 2M(x_i)}{2\pi S_0}\right), \tag{3.3}$$

where $M(\cdot)$ denotes an antiderivative of $\mu(\cdot)$.

Next, utilising the Cauchy–Schwarz inequality (2.11), the quantity $2\int_{t_i}^{t_f} \dot{x}_c{}^2 dt$ in (3.3) is bounded by

$$2\int_{t_i}^{t_f} \dot{x}_c{}^2 dt \geq \int_{t_i}^{t_f} \dot{x}_c{}^2 dt \geq \frac{(x_f - x_i)^2}{t_f - t_i}, \tag{3.4}$$

whereas combining (3.3) and (3.4) yields

$$\int_{t_i}^{t_f} L(x_c, \dot{x}_c)dt \geq \frac{1}{2\sigma^2}\left(\frac{(x_f - x_i)^2}{t_f - t_i} - b(t_f - t_i) - 2M(x_f) + 2M(x_i)\right). \tag{3.5}$$

https://doi.org/10.1017/S0956792518000530 Published online by Cambridge University Press

Thus, considering (2.9) and (3.5), an approximation for the response transition PDF of (2.3) was derived in [14] in the form

$$\hat{p}\left(x_f, t_f|x_i, t_i\right) = F(t_f|x_i, t_i)\exp\left(-G\left(x_f, t_f|x_i, t_i\right)\right), \tag{3.6}$$

where

$$G\left(x_f, t_f|x_i, t_i\right) = \frac{\left(x_f - x_i\right)^2 + \left(-2M(x_f) + 2M(x_i)\right)\left(t_f - t_i\right)}{2\left(t_f - t_i\right)\sigma^2}. \tag{3.7}$$

Note that the constant, for given t_i and t_f, term $\exp\left(\frac{-b(t_f - t_i)}{2\sigma^2}\right)$ has been merged with the constant F in (3.6) to be determined as

$$F(t_f|x_i, t_i) = \left(\int_{\mathcal{D}(M)} \exp\left(-G\left(y, t_f|x_i, t_i\right)\right) dy\right)^{-1}, \tag{3.8}$$

where $\mathcal{D}(M)$ denotes the domain of M.

It can be readily seen that $\hat{p} : \mathcal{D}(M) \times (t_i, +\infty) \times \{x_i\} \times \{t_i\} \to \mathbb{R}_+$ in (3.6) can be directly used as an analytical approximation of the response process PDF without resorting to the numerical solution of the E–L equation (2.8) and, thus, requires essentially zero computational effort for its determination. However, as demonstrated in [14], although the approximation of (3.6) is capable, in general, of capturing the salient features of the solution PDF, in many cases the degree of accuracy exhibited can be inadequate. In this regard, a more general form is proposed herein for the solution PDF, i.e.

$$\hat{p}_{(k,n)}\left(x_f, t_f|x_i, t_i\right) = F_{(k,n)}(t_f|x_i, t_i)\exp\left(-G_{(k,n)}\left(x_f, t_f|x_i, t_i\right)\right), \tag{3.9}$$

where

$$G_{(k,n)}\left(x_f, t_f|x_i, t_i\right) = \frac{k\left(x_f - x_i\right)^2 + n\left(-2M(x_f) + 2M(x_i)\right)\left(t_f - t_i\right)}{2\left(t_f - t_i\right)\sigma^2}, \tag{3.10}$$

and the constant F in (3.9) to be determined as

$$F_{(k,n)}(t_f|x_i, t_i) = \left(\int_{\mathcal{D}(M)} \exp\left(-G_{(k,n)}\left(y, t_f|x_i, t_i\right)\right) dy\right)^{-1}. \tag{3.11}$$

Note that the general solution form in (3.9) has two additional 'degrees of freedom', i.e. the parameters k and n to be determined based on an appropriate optimisation scheme as detailed in the following section. The rationale behind this choice relates to utilising available knowledge and integrating it in an optimisation scheme for enhancing the overall accuracy of (3.9). In particular, the parameter k relates to optimising and 'tightening' the Cauchy–Schwarz inequality of (3.4), whereas the parameter n refers to the overall accuracy of the WPI approximation of (2.9). In comparison to (3.6), it is anticipated that the approximation of (3.9) will exhibit higher accuracy, at the expense of course of some added modest computational cost related to the optimisation algorithm.

https://doi.org/10.1017/S0956792518000530 Published online by Cambridge University Press

3.2 Error minimisation and optimisation scheme

To determine the parameters k and n in (3.9), for a given norm ($\|\cdot\|_q$), the error quantity $\|\hat{p}_{(k,n)} - p^*\|_q$ is sought to be minimised, where p^* denotes the exact solution PDF. Nevertheless, since p^* is unknown, an alternative error minimisation scheme is adopted in the ensuing analysis based on the Fokker–Planck equation operator (see also [14] and references therein). Specifically, the exact transition PDF p^* for the SDE of (2.3) is given as the solution of the associated Fokker–Planck equation [24], i.e.

$$\frac{\partial p^*(x,t)}{\partial t} = -\frac{\partial\,(\mu(x)\,p^*(x,t))}{\partial x} + \frac{\sigma^2}{2}\frac{\partial^2 p^*(x,t)}{\partial x^2}. \tag{3.12}$$

Next, denoting the Fokker–Planck operator as

$$\mathcal{L}_{FP}[\,p(x,t)] = \frac{\partial p(x,t)}{\partial t} + \frac{\partial\,(\mu(x)\,p(x,t))}{\partial x} - \frac{\sigma^2}{2}\frac{\partial^2 p(x,t)}{\partial x^2}, \tag{3.13}$$

and considering that $\mathcal{L}_{FP}[\,p^*] = 0$, the error is defined as

$$err_q = \|\mathcal{L}_{FP}[\,\hat{p}_{(k,n)} - p^*]\|_q = \|\mathcal{L}_{FP}[\,\hat{p}_{(k,n)}] - \mathcal{L}_{FP}[\,p^*]\|_q = \|\mathcal{L}_{FP}[\,\hat{p}_{(k,n)}]\|_q. \tag{3.14}$$

Due to the analytical expression of $\hat{p}_{(k,n)}$, the error quantity $err_q = \|\mathcal{L}_{FP}[\,\hat{p}_{(k,n)}]\|_q$ can be explicitly determined as a function of k and n, see also [14]. In this regard, for a chosen q norm and final time t_f, the values of k, n are numerically evaluated by solving the optimisation problem

$$\hat{z}_q = \left(\hat{k}, \hat{n}\right)_q = \arg\min_{k,n\in\mathbb{R}} err = \arg\min_{k,n\in\mathbb{R}} \|\mathcal{L}_{FP}[\hat{p}_{(k,n)}(\cdot, t_f)]\|_q, \tag{3.15}$$

and, thus, the approximate response PDF of (3.9) is determined.

4 Examples

In the ensuing numerical examples, a standard interior point method [5, 17] using Matlab's *fmincon* built-in function is employed to solve the unconstrained optimisation problem of (3.15), in conjunction with the $\|\cdot\|_2$ norm. To this aim, the basic approximation of (3.6) with $(k,\, n) = (1,\, 1)$ serves as a natural choice for the initial starting point of the algorithm. Of course, in the current setting, the global minimum can be readily and directly identified by the three-dimensional plot of the corresponding objective function of (3.14) at minimal computational cost. However, the proposed numerical optimisation scheme has the additional merit that it can still be applied even in cases of potentially more sophisticated than (3.9) PDF approximations, where more than two parameters would need to be determined.

In all the numerical examples, the algorithm converged in less than approximately 50 iterations, which translates into a matter of few seconds from a computational cost perspective. The accuracy of the approximate PDF of (3.9) is demonstrated by comparisons to the PDF estimated based on pertinent MCS data (100,000 realisations) produced by numerically integrating the original equation (2.3).

https://doi.org/10.1017/S0956792518000530 Published online by Cambridge University Press

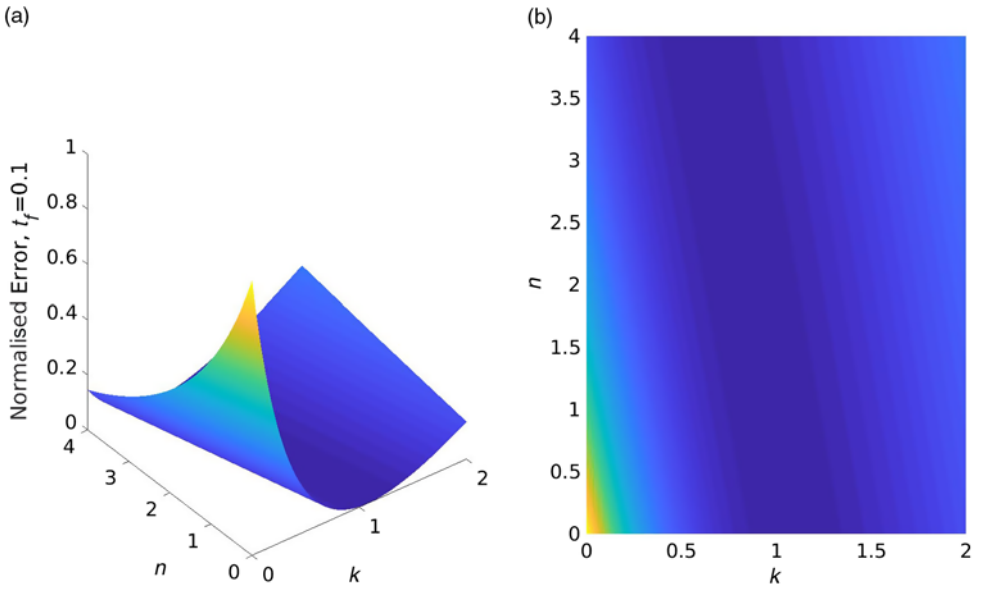

FIGURE 1. Example 4.1 objective function of (3.15) for $t_f = 0.1$.

4.1 Duffing kind nonlinearity: Hardening system

Consider the SDE of (2.3) with the hardening Duffing kind (e.g. [18]) nonlinear drift coefficient of the form

$$\mu(x) = -x - \lambda x^3. \tag{4.1}$$

In (4.1), λ is a parameter controlling the nonlinearity magnitude, whereas in the following, zero initial conditions are assumed, i.e. $X_0 = 0$, and the value $\sigma^2 = 2\pi S_0 = 1$. Taking into account that $M(x) = -\frac{x^2}{2} - \frac{\lambda}{4}x^4$, the PDF $\hat{p}_{(k,n)}$ of (3.9) takes the form

$$\hat{p}_{(k,n)}(x_f, t_f|0,0) = F(t_f|0,0)\exp\left(-\frac{kx_f^2 + n\left(x_f^2 + \frac{\lambda}{2}x_f^4\right)t_f}{2t_f}\right). \tag{4.2}$$

Next, utilising the parameter values $\lambda = 1$, $\sigma^2 = 2\pi S_0 = 1$, and applying the numerical optimisation scheme of (3.15) based on the $\|\cdot\|_2$ norm, yields the values for k and n. Specifically, in Figures 1 and 2, the objective functions of (3.14) are plotted for time instants $t_f = 0.1$ and $t_f = 1$, respectively, while in Table 1, the computed values of k and n are shown. In Figure 3, the approximate PDF $\hat{p}_{(k,n)}$ of (4.2) as well as the basic approximation $\hat{p}$ of (3.6) are plotted and compared with MCS-based estimated PDFs. It is seen that the herein proposed solution PDF approximation is in very good agreement with MCS data and yields enhanced performance as compared to the basic approximate PDF of (3.6).

4.2 Duffing kind nonlinearity: Bimodal response PDF

Consider next the SDE of (2.3) with the Duffing kind nonlinear drift coefficient of the form

$$\mu(x) = x - \lambda x^3. \tag{4.3}$$

https://doi.org/10.1017/S0956792518000530 Published online by Cambridge University Press

Table 1. *Computed* (k, n) *values for various final time instants* t_f *and starting point (1,1) for example 4.2*

	$t_f = 0.1$	$t_f = 1$
k	0.8957	0.3218
n	1.5981	1.8080

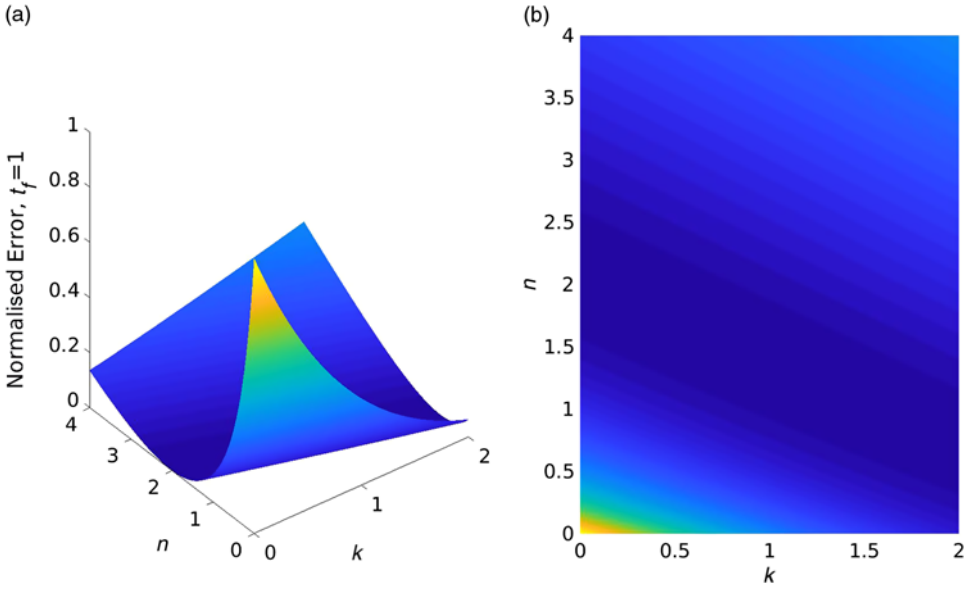

FIGURE 2. Example 4.1 objective function of (3.15) for $t_f = 1$.

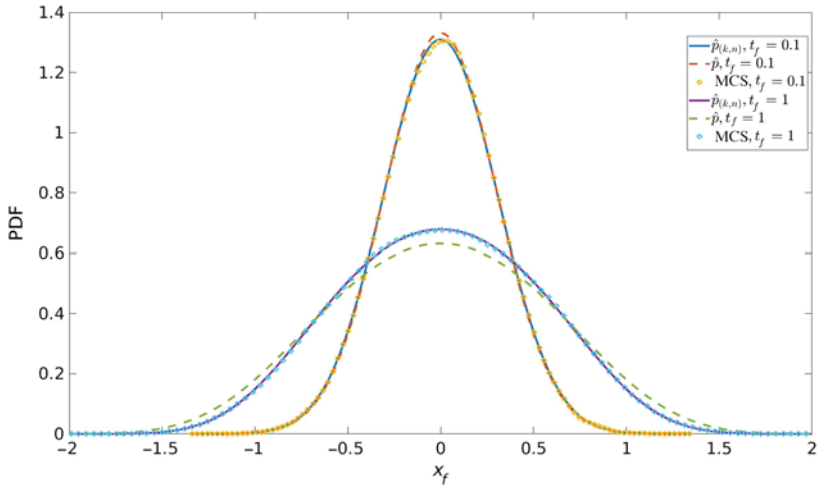

FIGURE 3. Approximate response PDFs $\hat{p}_{(k,n)}$ and $\hat{p}$ for a first-order hardening Duffing kind nonlinear SDE and comparisons with the MCS-based (100,000 realisations) PDF estimates.

https://doi.org/10.1017/S0956792518000530 Published online by Cambridge University Press

Table 2. *Computed* (k, n) *values for various final time instants* t_f *and starting point (1,1) for example 4.2*

	$t_f = 0.5$	$t_f = 5$
k	0.8253	1.2224
n	0.7373	1.4920

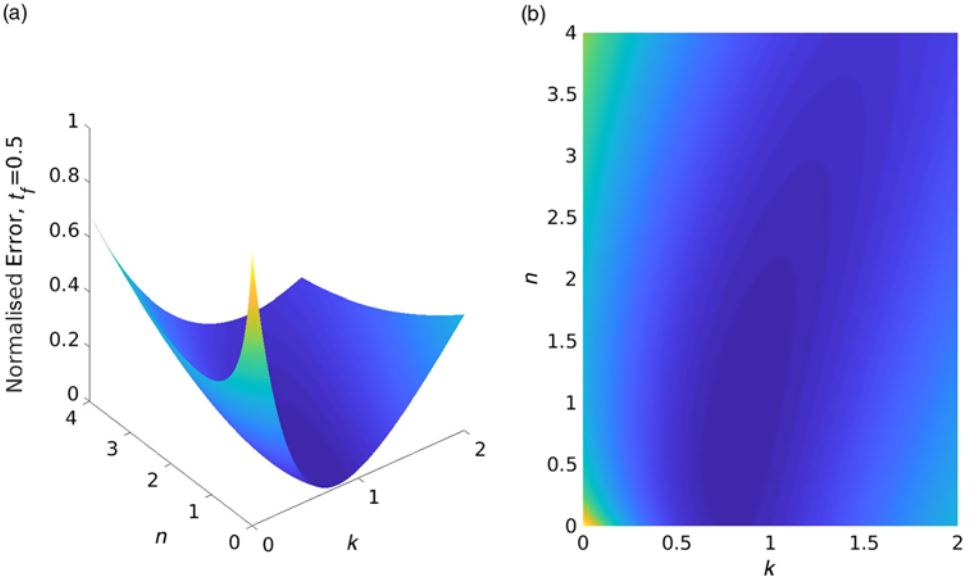

FIGURE 4. Example 4.2 objective function of (3.15) for $t_f = 0.5$.

Note that in comparison to (4.1), the nonlinearity form of (4.3) yields a bimodal response PDF for relatively large time instants t_f [18]. Thus, it can be argued that this bimodal PDF is more challenging to be estimated than the unimodal PDF corresponding to (4.1). Similarly as in (4.1), for zero initial conditions, (3.9) takes the form

$$\hat{p}_{(k,n)}(x_f, t_f|0, 0) = F(t_f|0, 0) \exp\left(-\frac{kx_f^2 + n\left(-x_f^2 + \frac{\lambda}{2}x_f^4\right)t_f}{2t_f}\right), \tag{4.4}$$

while for the parameter values $\lambda = 1, \sigma^2 = 2\pi S_0 = 1$, the objective functions of (3.14) are plotted for time instants $t_f = 0.5$ and $t_f = 5$ in Figures 4 and 5, respectively. In Table 2, the values of k and n, as determined by the numerical optimisation scheme, are shown, whereas in Figure 6 the approximate PDF $\hat{p}_{(k,n)}$ of (4.4) as well as the basic approximation $\hat{p}$ of (3.6) are plotted and compared with MCS-based estimated PDFs. It is readily seen that even in the relatively challenging case of the bimodal PDF, the herein proposed enhanced approximation is in very good agreement with MCS data and manages to capture the salient features of the PDF.

https://doi.org/10.1017/S0956792518000530 Published online by Cambridge University Press

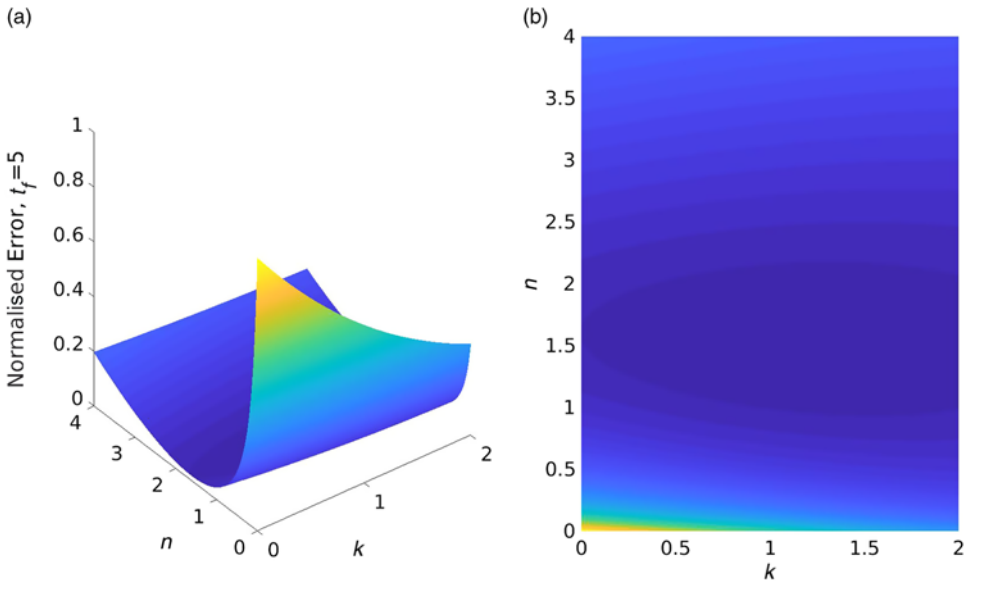

FIGURE 5. Example 4.2 objective function of (3.15) for $t_f = 5$.

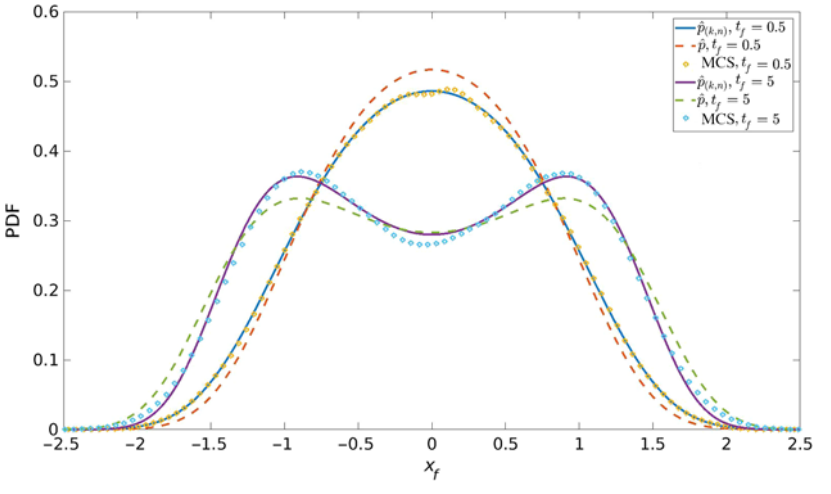

FIGURE 6. Approximate response PDFs $\hat{p}_{(k,n)}$ and $\hat{p}$ for a first-order bimodal Duffing kind nonlinear SDE and comparisons with the MCS-based (100,000 realisations) PDF estimates.

4.3 Haldane nonlinear stochastic equation

Consider next the SDE of (2.3) with the Haldane kind nonlinear drift coefficient of the form [19]

$$\mu(x) = -\frac{V_m x}{K_m + x + \frac{x^2}{K_i}}. \tag{4.5}$$

https://doi.org/10.1017/S0956792518000530 Published online by Cambridge University Press

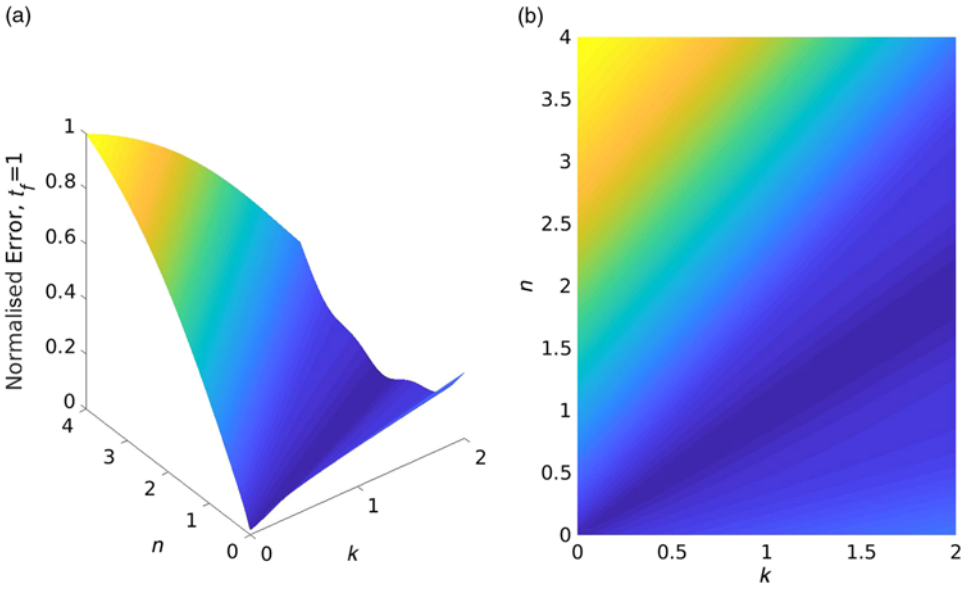

FIGURE 7. Example 4.2 objective function of (3.15) for $t_f = 1$.

This kind of modelling has been widely used to describe substrate inhibition kinetics and biodegradation of inhibitory substrates [19]. In (4.5), V_m and K_m denote the limiting rate and Michaelis constant, respectively, and K_i is the inhibition constant, while the process under consideration denotes the substrate concentration. In the following, the initial condition $X_0 = 10$ is considered and the parameter values $\sigma^2 = 2\pi S_0 = 0.01$ and $V_m = 1$, $K_m = 1$, $K_i = 20$, in accordance with [19]. Taking into account that $M(x) = -(5\sqrt{5}+10)\log(x+4\sqrt{5}+10) - (5\sqrt{5}+10)\log(x-4\sqrt{5}+10)$, the PDF $\hat{p}_{(k,n)}$ of (3.9) takes the form

$$\hat{p}_{(k,n)}(x_f, t_f|10, 0) = F(t_f|10, 0)\exp\left(-\frac{k\left(x_f-10\right)^2 + 2n\left(-M(x_f)+M(10)\right)t_f}{2t_f\sigma^2}\right). \tag{4.6}$$

In Figures 7–9, the objective functions of (3.14) are plotted for time instants $t_f = 1$, $t_f = 5$ and $t_f = 10$, respectively, while in Table 3, the computed values of k and n are shown. In Figure 10, the approximate PDF $\hat{p}_{(k,n)}$ of (4.6) as well as the basic approximation p_B of (3.6) are plotted and compared with MCS-based estimated PDFs. It is seen that although the accuracy of the basic approximation of (3.6) deteriorates for larger time instants t_f, the accuracy of the enhanced approximation of (3.9) remains in excellent agreement as compared to pertinent MCS data.

4.4 Oscillators with nonlinear damping

Consider a single degree-of-freedom oscillator with nonlinear damping whose motion is governed by

$$\ddot{y} + \beta\dot{y} + \omega_0^2 y + f(\dot{y}) = v(t), \tag{4.7}$$

https://doi.org/10.1017/S0956792518000530 Published online by Cambridge University Press

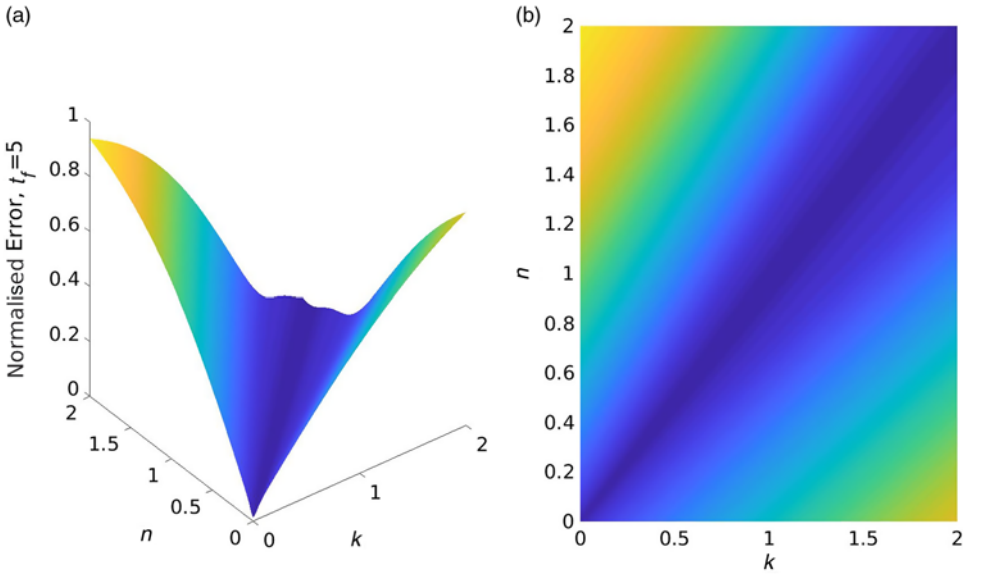

FIGURE 8. Example 4.2 objective function of (3.15) for $t_f = 5$.

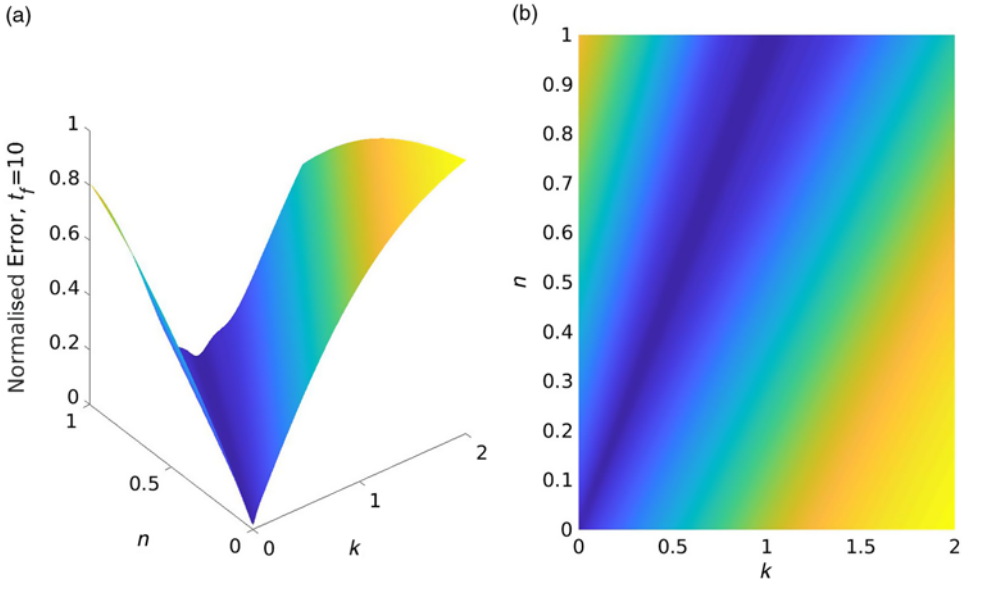

FIGURE 9. Example 4.2 objective function of (3.15) for $t_f = 10$.

where $f(\dot{y})$ is a nonlinear function depending on the response velocity and β is a linear damping coefficient, where $\beta = 2\zeta_0\omega_0$; ζ_0 is the ratio of critical damping and ω_0 is the natural frequency of the corresponding linear oscillator.

As shown in [10], a stochastic averaging/linearisation treatment can be applied to (4.7) and reduce the second-order SDE into a first-order SDE of the form of (2.3) governing the evolution in time of the response amplitude. Specifically, adopting the assumption of light damping, it can

https://doi.org/10.1017/S0956792518000530 Published online by Cambridge University Press

Table 3. *Computed* (k, n) *values for various final time instants* t_f *and starting point (1,1) for example 4.3*

	$t_f = 1$	$t_f = 5$	$t_f = 10$
k	0.9876	0.9698	0.7851
n	0.9787	0.9350	0.7688

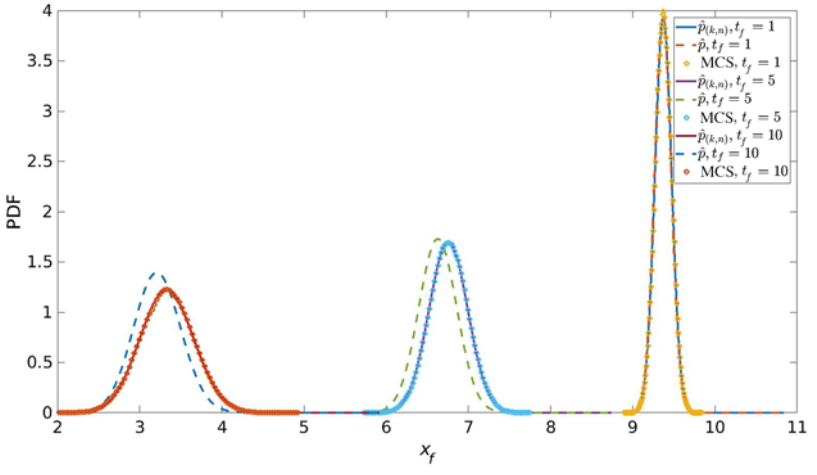

FIGURE 10. Approximate response PDF $\hat{p}_{(k,n)}$ and $\hat{p}$ for a Haldane kind nonlinear SDE and comparisons with the MCS-based (100,000 realisations) PDF estimates.

be argued that the nonlinear oscillator (4.7) exhibits a pseudo-harmonic behaviour described by the equations

$$y(t) = x\cos[\omega_0 t + \phi(t)] \tag{4.8}$$

and

$$\dot{y} = -\omega_0 x \sin[\omega_0 t + \phi(t)]. \tag{4.9}$$

In (4.8) and (4.9), x denotes the response amplitude defined as

$$x = \sqrt{y^2 + \frac{\dot{y}^2}{\omega_0^2}}, \tag{4.10}$$

whereas $\phi(t)$ denotes the response phase.

Assuming next that x is a slowly varying function with respect to time, a statistical linearisation treatment (e.g. [18]) yields an equivalent to (4.7) oscillator of the form

$$\ddot{y} + \beta(x)\dot{y} + \omega_0^2 y = v(t), \tag{4.11}$$

https://doi.org/10.1017/S0956792518000530 Published online by Cambridge University Press

where

$$\beta(x) = \beta + \frac{-\frac{1}{\pi}\int_0^{2\pi} \sin[\psi] f(-\omega_0 x \sin\psi) d\psi}{x\omega_0}. \tag{4.12}$$

Further, resorting to stochastic averaging (e.g. [9]), the response amplitude can be decoupled from the response phase, yielding a first-order SDE for the response amplitude x, i.e.

$$\dot{x} = -\frac{1}{2}\beta(x)x + \frac{\pi S_0}{2x\omega_0^2} + \frac{\sqrt{\pi S_0}}{\omega_0}\eta(t), \tag{4.13}$$

where $\eta(t)$ is a white noise process of unit intensity.

It can be readily seen that (4.13) is an SDE of the form of (2.3) with drift μ and diffusion σ coefficients given by

$$\mu(x) = -\frac{1}{2}\beta(x)x + \frac{\pi S_0}{2x\omega_0^2} \tag{4.14}$$

and

$$\sigma = \frac{\sqrt{\pi S_0}}{\omega_0}, \tag{4.15}$$

respectively. As an illustrative example, the linear plus cubic damping oscillator

$$\ddot{y} + \beta\dot{y}(1 + \epsilon\dot{y}^2) + \omega_0^2 y = v(t) \tag{4.16}$$

is considered next. For this case, (4.2) becomes

$$\beta(x) = \beta\left(1 + \epsilon\frac{3}{4}\omega_0^2 x^2\right). \tag{4.17}$$

In (4.17), ϵ is a parameter controlling the nonlinearity magnitude, whereas in the following, the initial conditions, $y(t_i = 0) = 1$, $\dot{y}(t_i = 0) = 0$, and the parameter values $\left(\omega_0 = 1, \zeta_0 = 0.01, S_0 = \frac{6}{\pi}\zeta_0\right)$ are considered. Next, taking into account that $M(x) = -\frac{\beta}{2}\left(\frac{x^2}{2} + \epsilon\frac{3}{16}\omega_0^2 x^4\right) + \frac{\pi S_0}{2\omega_0^2}\log(x)$, the PDF of (3.9) for oscillator response amplitude takes the form

$$\begin{aligned}&\hat{p}_{(k,n)}(x_f, t_f|1, 0)\\ &= F(t_f|1, 0)\exp\left(-\frac{k\left(x_f - 1\right)^2 + n\left(\beta\left(\frac{x_f^2}{2} + \epsilon\frac{3}{16}\omega_0^2 x_f^4 - \frac{1}{2} - \epsilon\frac{3}{16}\omega_0^2\right) - \frac{\pi S_0}{\omega_0^2}\log(x_f)\right)t_f}{2t_f\frac{\pi S_0}{\omega_0^2}}\right),\end{aligned} \tag{4.18}$$

while for the parameter value $\epsilon = 3$, the objective functions of (3.14) are plotted for time instants $t_f = 3$ and $t_f = 40$ in Figures 11 and 12, respectively. In Table 4, the values of k and n as determined by the numerical optimisation scheme are shown, whereas in Figure 13, the approximate PDF $\hat{p}_{(k,n)}$ of (4.18) as well as the basic approximation $\hat{p}$ of (3.6) are plotted and compared with MCS-based estimated PDFs. It is readily seen that even in this relatively challenging case of a linear plus cubic damping oscillator, the herein proposed enhanced approximation is in very good agreement with MCS data and manages to capture the salient features of the PDF.

https://doi.org/10.1017/S0956792518000530 Published online by Cambridge University Press

Table 4. *Computed* (k, n) *values for various final time instants* t_f *and starting point (1,1) for example 4.4*

	$t_f = 3$	$t_f = 40$
k	0.4076	6.5478
n	2.0611	0.3817

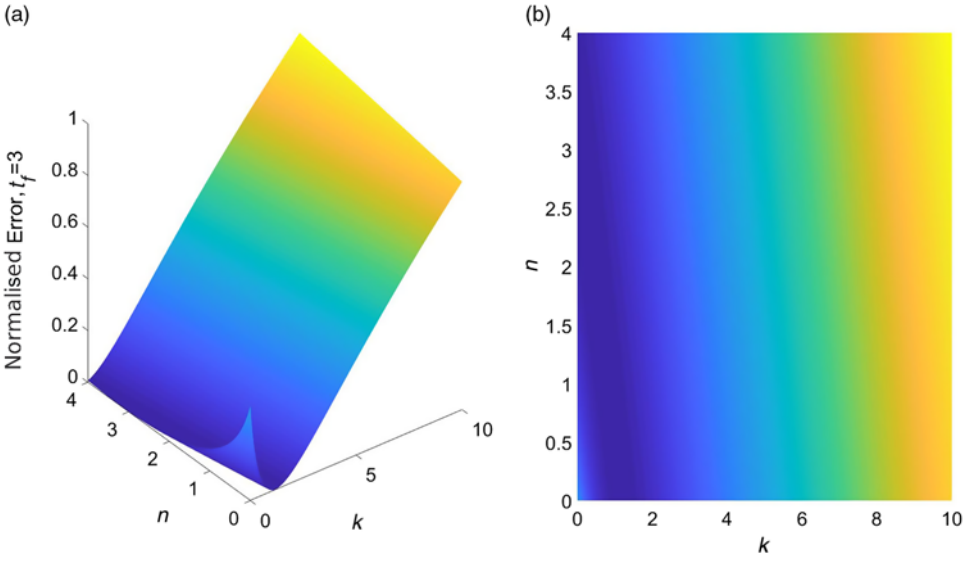

FIGURE 11. Example 4.4 objective function of (3.15) for $t_f = 3$.

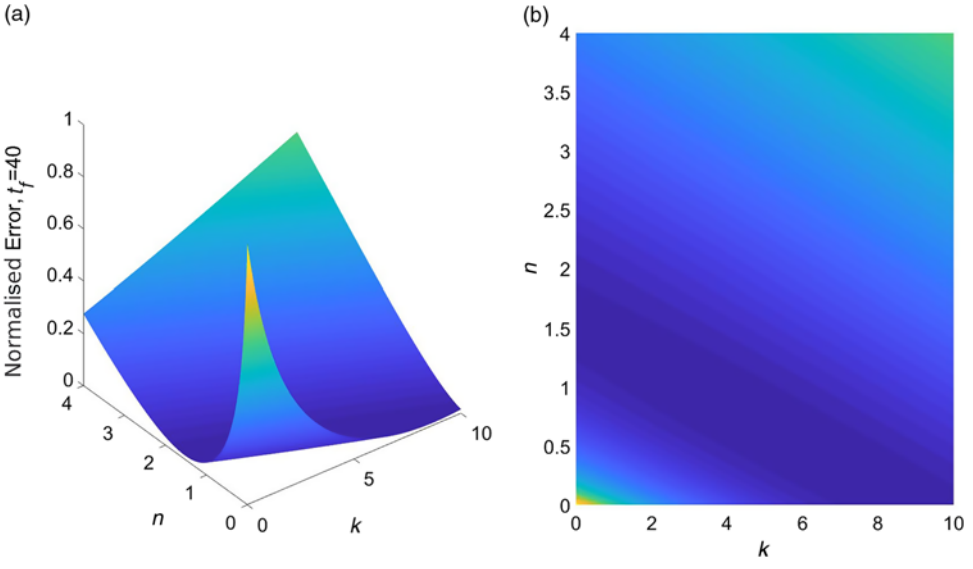

FIGURE 12. Example 4.4 objective function of (3.15) for $t_f = 40$.

https://doi.org/10.1017/S0956792518000530 Published online by Cambridge University Press

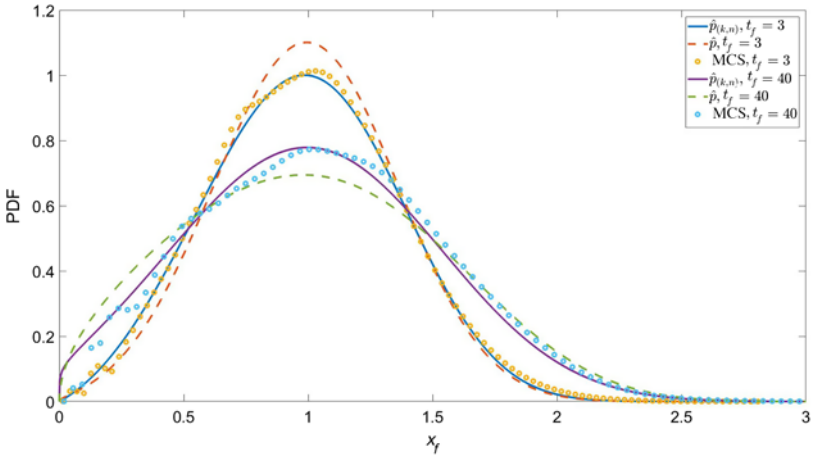

FIGURE 13. Approximate response PDFs $\hat{p}_{(k,n)}$ and $\hat{p}$ for a linear plus cubing damping oscillator and comparisons with the MCS-based (100,000 realisations) PDF estimates.

5 Conclusion

In this paper, an approximate analytical expression for the response transition PDF of a class of SDEs with constant diffusion, but nonlinear drift coefficients, has been derived based on the concept of the WPI and on a Cauchy–Schwarz inequality treatment. This has been done in conjunction with formulating and solving an error minimisation problem by relying on the associated Fokker–Planck equation operator. In comparison to the basic approximation proposed in [14], the herein derived approximate PDF exhibits enhanced accuracy as demonstrated by pertinent MCS data. Overall, a closed form approximate analytical solution PDF has been derived at minimal computational cost, which can serve also as a benchmark for assessing the performance of alternative, more computationally demanding, stochastic dynamics numerical methodologies.

Acknowledgement

I. A. Kougioumtzoglou gratefully acknowledges the support through his CAREER award by the CMMI Division of the National Science Foundation, USA (award number: 1748537).

Conflict of interest

None.

References

[1] CHAICHIAN, M. & DEMICHEV, A. (2001) *Path Integrals in Physics: Volume I Stochastic Processes and Quantum Mechanics*, CRC Press, Bath, UK.

[2] DI MATTEO, A., KOUGIOUMTZOGLOU, I. A., PIRROTTA, A., SPANOS, P. D. & DI PAOLA, M. (2014) Stochastic response determination of nonlinear oscillators with fractional derivatives elements via the Wiener path integral. *Prob. Eng. Mech.* **38**, 127–135.

[3] EWING, G. M. (1969) *Calculus of Variations with Applications*, Dover Publications, New York, USA.

https://doi.org/10.1017/S0956792518000530 Published online by Cambridge University Press

[4] FEYNMAN, R. P. (1948) Space-time approach to non-relativistic quantum mechanics. *Rev. Modern Phys.* **20**(2), 367.
[5] FORSGREN, A., GILL, P. E. & WRIGHT, M. H. (2002) Interior methods for nonlinear optimization. *SIAM Rev.* **44**(4), 525–597.
[6] GRIGORIU, M. (2002) *Stochastic Calculus: Applications in Science and Engineering*, Springer Science & Business Media, New York, USA.
[7] KAY, S. M. (1993) *Fundamentals of Statistical Signal Processing: Estimation Theory*, Prentice Hall PTR.
[8] KOUGIOUMTZOGLOU, I. A. (2017) A Wiener path integral solution treatment and effective material properties of a class of one-dimensional stochastic mechanics problems. *ASCE J. Eng. Mech.* **143**(6), 04017014, 1–12. doi:10.1061/(ASCE)EM.1943-7889.0001211.
[9] KOUGIOUMTZOGLOU, I. A. & SPANOS, P. D. (2009) An approximate approach for nonlinear system response determination under evolutionary stochastic excitation. *Curr. Sci.* **97**(8), 1203–1211.
[10] KOUGIOUMTZOGLOU, I. A. & SPANOS, P. D. (2012) An analytical Wiener path integral technique for non-stationary response determination of nonlinear oscillators. *Prob. Eng. Mech.* **28**, 125–131.
[11] KOUGIOUMTZOGLOU, I. A. & SPANOS, P. D. (2014) Nonstationary stochastic response determination of nonlinear systems: a Wiener path integral formalism. *ASCE J. Eng. Mech.* **140**(9), 04014064, 1–14. doi:10.1061/(ASCE)EM.1943-7889.0000780.
[12] KOUGIOUMTZOGLOU, I. A., DI MATTEO, A., SPANOS, P. D., PIRROTTA, A. & DI PAOLA, M. (2015) An efficient Wiener path integral technique formulation for stochastic response determination of nonlinear MDOF systems. *ASME J. Appl. Mech.* **82**(10), 101005.
[13] LI, J. & CHEN, J. (2009) *Stochastic Dynamics of Structures*, John Wiley & Sons, (Asia) Pte Ltd.
[14] MEIMARIS, A. T., KOUGIOUMTZOGLOU, I. A. & PANTELOUS, A. A. (2018) A closed form approximation and error quantification for the response transition probability density function of a class of stochastic differential equations. *Prob. Eng. Mech.*, **54**, 87–94. doi:10.1016/j.probengmech.2017.07.005.
[15] MUKHOPADHYAY, N. (2000) *Probability and Statistical Inference*, Marcel Dekker Inc, New York, USA.
[16] NAESS, A. & JOHNSEN, J. M. (1993) Response statistics of nonlinear, compliant offshore structures by the path integral solution method. *Prob. Eng. Mech.* **8**(2), 91–106.
[17] NOCEDAL, J. & WRIGHT, S. J. (1999) *Numerical Optimization*, Springer, New York, USA.
[18] ROBERTS, J. B. & SPANOS, P. D. (2003) *Random Vibration and Statistical Linearization*, Courier Corporation, New York, USA.
[19] SONNAD, J. R. & GOUDAR, C. T. (2004) Solution of the Haldane equation for substrate inhibition enzyme kinetics using the decomposition method. *Math. Comput. Model.* **40**(5–6), 573–582.
[20] SPANOS, P. D., KOUGIOUMTZOGLOU I. A., DOS SANTOS K. R. M. & BECK A. T. (2018) Stochastic averaging of nonlinear oscillators: Hilbert transform perspective. *ASCE J. Eng. Mech.* **144**(2), 04017173, 1–9.
[21] STEELE, J. M. (2004) *The Cauchy–Schwarz Master Class: An Introduction to the Art of Mathematical Inequalities*, Cambridge University Press, New York, USA.
[22] TANIGUCHI, T. & COHEN, E. G. D. (2008) Inertial effects in nonequilibrium work fluctuations by a path integral approach. *J. Stat. Phys.* **130**(1), 1–26.
[23] TOUCHETTE, H. (2009) The large deviation approach to statistical mechanics. *Phys. Rep.* **478**, 1–69.
[24] VAN KAMPEN, N. G. (1992) *Stochastic Processes in Physics and Chemistry*, Elsevier, New York, USA.
[25] WEHNER, M. F. & WOLFER, W. G. (1983) Numerical evaluation of path-integral solutions to Fokker–Planck equations. II. Restricted stochastic processes. *Phys. Rev. A* **28**, 3003.
[26] WIENER, N. (1921) The average of an analytic functional and the Brownian movement. *Proc. Natl Acad. Sci.* **7**(10), 294–298.